ROAD EXTRACTION AND ENVIRONMENT INTERPRETATION FROM LIDAR SENSORS

Laurent Smadja, Jérôme Ninot and Thomas Gavrilovic

VIAMETRIS, Maison de la Technopole, 6 rue Leonard de Vinci, BP0119, 53001 Laval cedex, France, www.viametris.fr

Commission III, WG III/2

KEY WORDS: LIDAR / Camera calibration, Unsupervised road extraction, Interpreted 3D reconstructions

ABSTRACT:

We present in this article a new vehicle dedicated to road surveying, equipped with a highly precise positioning system, 2D lidar scans and high definition color images. We focus at first on the sensors extrinsic calibration process. Once all sensors have been positioned in the same coordinates system, 3D realistic environments can be computed and interpreted. Moreover, an original algorithm for road extraction has been developed. This two-step method is based on the local road shape and does not rely on the presence of curbs or guardrails. Different uses of the RanSaC algorithm are employed, for road sides rough estimation in the first place, then for unlikely candidates elimination. Road boundary and center points are further processed for road width and curvature computation in order to feed a geographic information system. Finally, a simple extraction of traffic signs and road markings is presented.

1 INTRODUCTION

Road administrators require more and more objective informations about their network and its surrounding environment for various purposes : disaster management, urban planning, tourist guidance or simply road network management are some of the applications that demand precise city modeling and interpretation. Industry also needs 3D reconstructions of large areas ; map providers for navigation systems now include semantic data in their bases that can be interfaced in warning or driving assistance systems, mobile communication development needs data for radio waves coverage analysis *etc.* These are few examples among many fields that need augmented digital maps. Many companies and research labs have then focused in the last decade on the acquisition of mass data, developing many acquisition platforms. Road network surveying generally implies aerial or satellite multi spectral images processing but these approaches suffer from a lack of precision regarding road geometry, although they provide a good classified overview of processed areas (Hatger and Brenner, 2003) (Samadzadegan et al., 2009). Some research teams have therefore promoted fusion between terrestrial and aerial data (Früh and Zakhor, 2004), requiring an existing digital elevation map of the area to be processed. City modeling is generally performed by means of vehicle borne lidar and cameras (Zhao and Shibasaki, 2003) (Deng et al., 2004) (Boström et al., 2006) ; these works however do not apply on road geometry or characterization. Some companies, cartographic institutes and laboratories developed road dedicated vehicles, using inertial systems and 3D lidar sensors in order to provide interpreted road environments. StreetMapper (Barber et al., 2008) focus on elevation models, ICC (Talaya et al., 2004) use stereo and (Ishikawa et al., 2006) monocular images for automatic processes, finally (Jaakkola et al., 2008) process lidar data as image for extracted different kinds of road markings. (Goulette et al., 2006) only provide automatic lidar data segmentation, performing classification of acquired scans in road, trees or obstacles. The acquisition speed is nevertheless very low and the developed method can not deal with rural roads, as road extraction implies curbs.

From our point of view, there were no current solution offering a full comprehension of road environment, gathering road geometry, road marking and traffic sign analysis in a single tool. This is the purpose of our developments, while we focus here on road extraction and applications from lidar data.

2 VEHICLE DESIGN AND CALIBRATION

We developed an acquisition vehicle for road surveying consisting in a very precise positioning system, a CCD Color camera and 4 linear scanning sensors. A brief description of these sensors and the calibration methods is provided in this section.

2.1 Vehicle Specification

The positioning system consists in a Trimble Omnistar 8200-Hp GPS receiver, combined with an Ixsea LandINS inertial measurement unit. This association delivers filtered 200 Hz GPS data and can support GPS outages up to $300s$ while presenting very small drifts (0.005° for pitch and roll, 0.01° for heading, 0.7m in the xy plane and 0.5m for the z coordinate). Orientation data are given in a North East Up reference, and GPS positions are translated in a metric coordinates system using the adequate conic projection.

As an imaging system, we use an AVT Pike F-210C, a CCD color camera which provides Bayer filtered high definition images, with a frame rate up to 30 Hz. Instead of a constant rate, we decided to set the camera such as it takes an image every n meters (n is generally set to 5 m, but can be adapted depending on environment).

Four SICK LMS-291 are installed on the roof of the vehicle (Cf. figure 1(a)). These Laser range sensors provide 180° scans (with 0.5° angular resolution) up to 60 Hz scan rate. Their sensing maximum range reaches 80 m with a 10 mm error and they also can output reflectivity values (Cf. figure 6). Three of them are looking to the ground with different orientations, the fourth one being oriented towards the sky, in order to capture building facades or trees (Cf. figure 1(b)). These sensors are controlled by the vehicle speed, stopping the acquisition when the vehicle is stopped.

Every data are acquired and timestamped using $^{\text{RT}}$Maps software, on a single on-board computer (Pentium IV, 2GHz) with adequate disk space. Besides, considering the inertial navigation system

(a) Lidar and camera

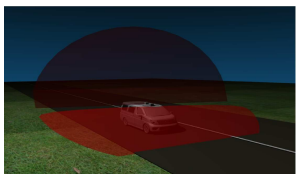

(b) "Front" and "Sky" lidar sensors cones of view

Figure 1: overview of the truck

(and more specifically the GPS antenna position) as the center of the truck coordinates system, every data have to be replaced in this specific frame, and will be finally expressed in the world coordinates system. We now present briefly the calibration methods used for replacing all devices in this coordinates system.

2.2 Camera Calibration

We present in this section a two step camera calibration ; first the camera is roughly oriented so as to be aligned with the truck main axis. Then it is finely calibrated, using a dedicated Matlab toolbox.

2.2.1 Camera Rough Alignment We designed a calibration site presenting many parallel longitudinal and transversal lines and marks for positioning the vehicle wheels. A primary camera orientation is processed in order to align it with the truck main axis : it consists in a dynamic process allowing a rough setting of the pitch, the roll and the yaw. Pitch is set in a way that the vehicle's hood is not seen. Roll is set to zero from the transversal lines mean orientation. Yaw is set so that the longitudinal lines vanishing point has an u-coordinate equals to the principal point – *i.e.* the projection of the camera center in the image – u-coordinate (Cf. figure 2).

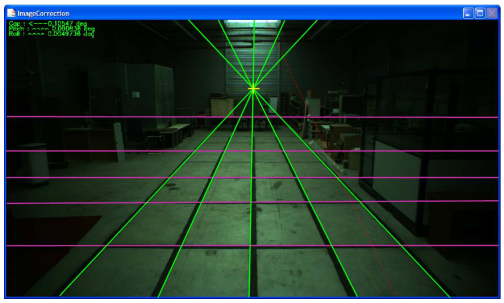

Figure 2: configuration tool output image, instructions are displayed at the top left of the image

2.2.2 Fine Calibration We mainly focus here on extrinsic calibration, *i.e.* the camera position and orientation with respect to the truck. We used Jean-Yves Bouguet's Matlab camera calibration toolbox [1], which relies on Zhang calibration algorithm (Zhang, 2000) and returns calibration grid positions in the camera coordinates system (Cf. figure 3).

Intrinsic parameters, though quite important for any image processing algorithm, are not critical in the road description process. Indeed, this first stage goal is to define camera position and orientation in the GPS antenna coordinates system, which is done using our calibration site.

[1] `http://www.vision.caltech.edu/bouguetj/calib_doc/index.html`

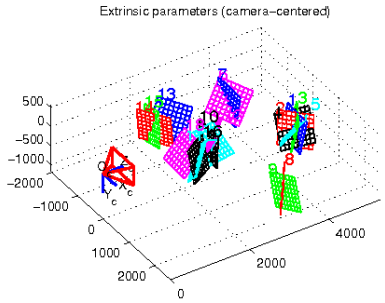

Figure 3: calibration grid positions

2.3 Lidar Calibration

In order to compute Lidar positions and orientations in the GPS coordinates system, we decided to determine their positions with respect to the camera, then to transfer these positions using the camera extrinsic calibration results.

Different approaches for lidar calibration have been developed. Antone and Friedman implemented a method where only lidar range data are required, but which is based on the design of a specific calibration object (Antone and Friedman, 2007). They claim that registration to any camera can be further processed by applying a pattern on this object. (Mählisch et al., 2006) developed a calibration method of a multi-beam lidar sensor with respect to a camera which has to be sensitive to the spectral emission band. Alignment is then performed when viewing a wall from different orientations, through a reprojection distance minimization. Huang presented an algorithm for multi-plane lidar calibration using geometric constraints on the calibration grid plane (Huang and Barth, 2008). We chose Zhang and Pless approach (Zhang and Pless, 2004), a two step algorithm based on a geometric constraint relative to the normal of the calibration grid plane. This method uses a linear determination of the pose parameters, further refined by a non linear optimization (generally performed through a Levenberg-Marquardt algorithm).

In our experiments, we use about 15 images, where the calibration grid is seen in both lidar and camera views. The poses of the calibration grid with respect to the camera are previously determined in the 2.2.2 section and we select manually the grid area in the lidar scan (Cf. figure 4). Zhang and Pless two-pass algorithm is then performed with the collected data for the three front lidar range sensors.

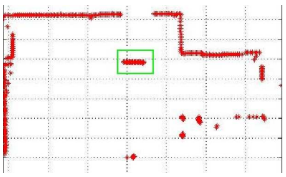

(a) Calibration grid is manually selected in the scan

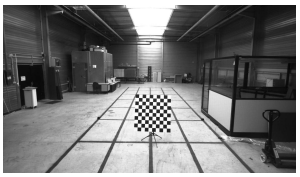

(b) corresponding image

Figure 4: lidar data and corresponding image used for calibration

As an intermediate result of this stage, we can reproject lidar impacts on the grid, as can be seen in figure 5.

The final step in the calibration scheme consists in replacing all calibrated lidar in the GPS antenna coordinates system, in order to have all sensors in the same reference. As these sensors are 2D lidar, the vehicle displacement provides a full scan of the surrounding 3D world. Using ^{RT}Maps acquisition platform, all data

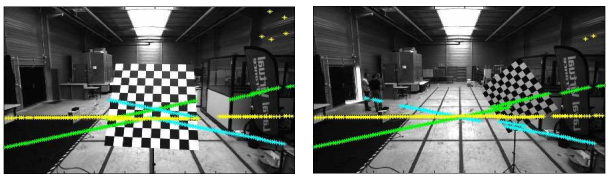

Figure 5: lidar impacts reprojected on the calibration grid

are timestamped, then can be positioned through a linear interpolation of the GPS-INS positions data. Consistent 3D environments can thus be constructed from the four 2D lidar sensors (Cf. figure 6) when driving at a *normal speed*.

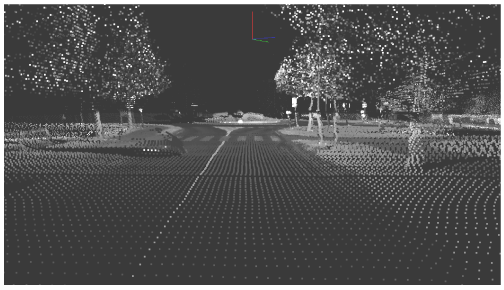

Figure 6: 3D world with reflectivity data

Moreover, using lidar camera calibration, it is possible to texturize all lidar points, and thus to render realistic 3D reconstructions (Cf. figure 7).

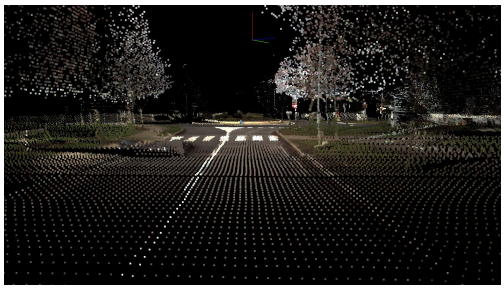

Figure 7: same view with texture information

3 ROAD EXTRACTION

To our knowledge, there are few road boundaries detection methods using only lidar range sensors. A well known paper (Kirchner and Heinrich, 1998) settles an horizontal lidar in order to detect guardrails. A third polynomial road boundary model (with no first order term) is used to approximate clothoid curve and an extended Kalman filter processes successive scans. The Kalman prediction is performed using the steering angle and vehicle speed and the correction stage assumes a radial error model. This approach inspired many other research teams despite of being limited to roads presenting guardrails or curbs : another method uses a lidar oriented towards the road and looks for curbs in successive scans (Wijesoma et al., 2004). They assumed that each scan is ideally composed with different "flat" phases : horizontal as the sidewalks and the road, vertical as the curbs borders. A predicted point is computed from the previous two range measurements on a frame, large prediction errors indicating phase changes. The extracted segments are fitted by lines then further analyzed to provide potential curbs. Final detections are tracked using an extended Kalman filter. The "flat road" approach has also been tested by (Kim et al., 2007), that ensure a robot positioning through a curb detection. Noticing that, due to the larger point density in front of the range sensor, the most represented line is the road, they performed a Hough Transform on the scan data. Curbs are then extracted as the extrema points surrounding the road. An apparently faster approach uses histogram thresholding to detect curbs (Aufrere et al., 2003), from a side oriented lidar sensor, and *via* a modular algorithm. A maximum contrast approach is then used as curbs present a different illumination than road and sidewalk. Different approaches use a multi-layer lidar sensor. (Dietmayer et al., 2006) presents two aspects of road detection with an 6 layers lidar, two of them being dedicated to lane following; this part is performed by correctly setting the sensor sensitivity, as asphalt present a small reflectivity compared to road markings. Besides, they present an object detection by segmenting each scan with an adaptive threshold, the classification being performed through the object dynamic analysis (Sparbert et al., 2001). These obstacles are further eliminated so as not to disturb the road extraction process. Assuming an equal curvature for left and right sides and considering several curvature hypotheses, the road is extracted by finding the solution that minimizes the number of candidates between the road boundaries. The authors finally classify the road type from the estimated width, and discard unlikely object classifications.

Starting from the observations we made, we developed a two-step road detection algorithm which processes the front lidar scans. This algorithm, based on different uses of RanSaC method (Fischler and Bolles, 1981), is described in this section. Extracted road boarders and centers are then processed and provide useful information about road geometry, such as road width or road curvature.

3.1 Scan Rough Segmentation

In the first step, each scan is processed individually. Looking at figures 8(a) and 8(b), where scan points are reprojected in the world coordinates system, it can be noticed that the road is not flat, but verifies a curvature which can be approximated quite accurately by a parabola. This is the starting point of our algorithm : it is to find a polynomial expression, up to degree 2 that best approximates the scan data. Using RanSaC algorithm, only two thresholds are necessary ; the first one indicates the expected outliers rate in the points set, which is directly related to the iterations number, and the second one specifies the distance above which a point is considered as an outlier.

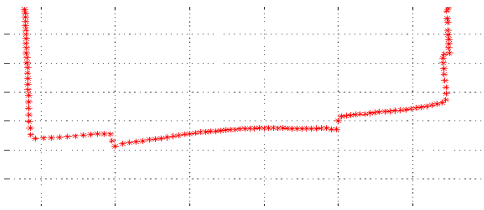

(a) urban road with curb

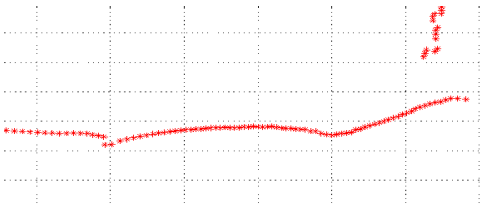

(b) rural road

Figure 8: two typical road scans where road local

The scan segmentation results are presented on figures 9(a) and 9(b). It can be seen that the road is well extracted, although some points could be wrongly classified, as they fortuitously belong to the best parabola. A simple morphological erosion is then performed on the inliers indices vector in order to discard isolated positive points.

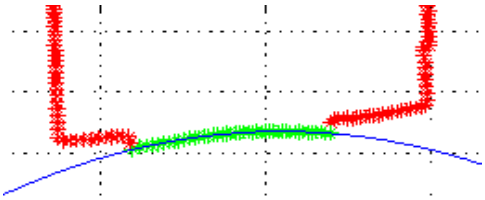

(a) rough urban road segmentation

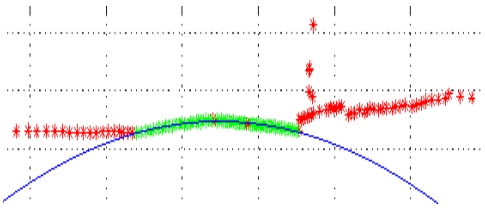

(b) rural road segmentation

Figure 9: scan rough segmentation : Inliers are displayed in green

We believe that this approach is quite efficient as it does not rely on the presence of curbs, guard rails or concrete steps, but simply assumes that there exists a main polynomial corresponding to the road. As can be seen on image 10, this first step classifies quite well road to non road points. Nevertheless, two remarks could be formulated :

- This approach will fail when the sidewalks are larger than the road, more precisely when they represent more points than the road. In this very case, sidewalks will be detected as the main polynomial, then classified as road. This limitation will be addressed in the section 3.2.
- The results look very noisy. Indeed, no global consistency has been used yet.

3.2 Slope Break Points

We saw in the previous section that large sidewalks could lead to wrong road extraction. This eventuality is quite rare as the front lidar points density is higher in front of the truck (*i.e.* on the road), but can sometimes occur when riding on a narrow road or on rural roads. The lidar scan can thus be pre-segmented in order to decrease these cases frequency, using slope break points.

A very interesting approach of city and road modeling is described in (Goulette et al., 2006), where the authors present a geometric adaptive decimation. This process greatly reduces the lidar data by keeping geometrically meaningful points only. Following the same way, we decided to segment each lidar by detecting slope break points, *i.e.* points where slope change significantly (the significance threshold being around 30°). These points generally occur at curbs boundaries, in vegetation areas, but *not* on the road surface. Once these break points have been detected, the RanSaC parabola algorithm is successively performed on each segment defined between two such points (if the segment in question has enough points) ; the segment presenting the greatest inliers numbers is finally kept. This process presents two main advantages :

- It separates large sidewalks in two parts
- It decreases the number of points number for each RanSaC application. This speeds up the process as a large number of points is very time consuming.

The output of this step is a first road/non-road classification of lidar points (Cf. figure 10). At that point, road boundaries are simply defined as the extreme positive points. Road mid points are also computed, as they constitute an interesting information, from the middle of left and right boundaries.

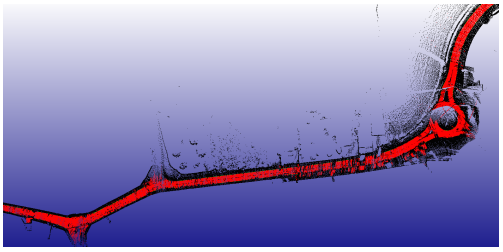

Figure 10: first stage result : road points are displayed in red

3.3 Global Consistency

We showed in the previous section how to discard false positives in road classification, using a simple geometric constraint. But even after this process, the road extraction is not precise enough, curvature and width would be very noisy if determined at this point. We propose here a more global approach, that provides "confidence" scores to the left road side, right road side and middle points extracted in the first stage.

This algorithm uses the RanSaC method combined to an accumulation scheme and can be resumed as follows for a particular side :

1. At the beginning of the algorithm, each point has a zero confidence score.
2. For standard acquisition conditions (around 90 km.h^{-1} with a 60 Hz lidar), the linear resolution is about 50 cm. The starting point of our algorithm is to pick N consecutive points and discard their z coordinate. We choose generally $N = 100$, that corresponds to 50 m, as the road can not change that fast.
3. These points are oriented in order to be fitted by a third order polynomial $y = f(x)$, as this type of function is able to correctly approximate a clothoid.
4. We apply RanSaC algorithm, but we are more interested in the inliers indices than by the polynomial. Indeed, the confidence score of each inlier is increased.
5. Go forward by S points and iterate from (2).

After all processes, each candidate point has a confidence score from 0 to $\frac{N}{S}$, depending of the number of times it has been considered as an inlier. Finally, a road side candidate is kept if its score is above a threshold. The result of this step can be seen on figure 11, where score color goes from dark blue (0) to red (10).

Three independent polynomials $y = f(x)$ are instanced, for left, right and center points, so as to handle unsymmetrical road sides.

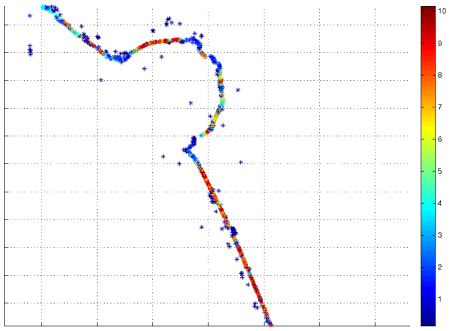

Figure 11: scores for mid points candidates

The output points will be further fitted by a Non Uniform Rational Bézier Spline (called NURBS hereafter). Using scores as weights in NURBS computations seemed at first a good idea, but as even a small weight influences the final curve, the threshold approach has been preferred.

3.4 NURBS Fitting

Due to the algorithm architecture, road boundary candidates are generally quite sparse and irregularly spaced, so a simple linear interpolation between them would not be satisfying. Resultant points are thus approximated by 3D NURBS, parametric curves whose resolution is directly related to the distances between successive knots (Cf. figure 12(a)). Applying algorithm described in (Peterson, 1992), we output 3D curves with a constant arc-length spacing (Cf. figure 12(b)). This method is based on spline arc-length estimation, using Gauss-Legendre quadrature and Newton's root finding method.

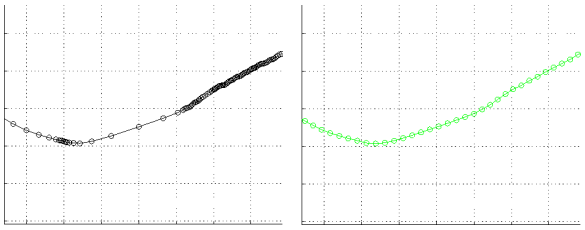

(a) original NURBS (b) arc-length NURBS

Figure 12: after reparametrization, curve points are equally spaced

4 APPLICATIONS

4.1 Road curvature estimation

Using the NURBS computed in section 3.4, it is almost straightforward to determine road curvature with any desired resolution. We chose a 50 cm resolution on the central NURBS, and computed the circle from three successive points. Two results can be seen on figures 13(a) and 13(b), where point color changes from green to red when the curvature increases. Hazardous areas can thus be detected and precisely reported on a geographic information system.

4.2 Road width estimation

In the same manner as in section 4.1, we chose a 50 cm resolution on the central NURBS, and computed at each point the curve normal plane, reminding that we deal with 3D curves. It is then to find the intersections between this plane and the left and right splines to obtain the left and right boundaries. Following the same path than in section 3.4, we applied the Newton's method, in order to minimize the distance between the plane and the boundary splines. The minimization starting point is here crucial and has to be carefully computed.

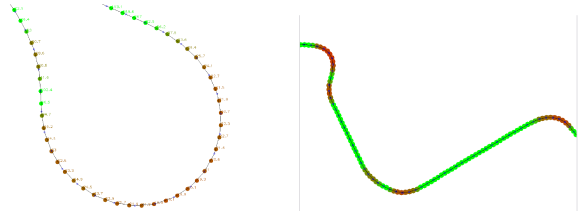

Figure 13: road curvature estimation for two different areas

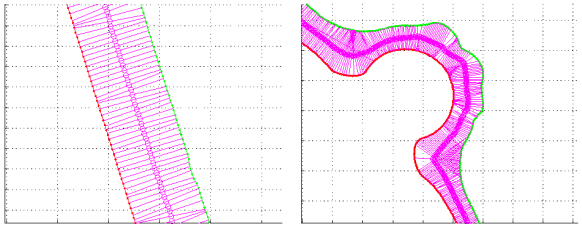

Figure 14: two examples of road width

4.3 Road signs extraction

Road signs are designed to present a high reflectivity ; on image 6, where the points reflectivity is displayed as a gray level, we can observe white areas, corresponding to license plates or road signs. Using a simple threshold on reflectivity value then on the size of the resulted areas, we can easily extract road signs in the virtualized environments (Cf. figure 15). The sign areas can further be reprojected on image in order to perform optical fine extraction and recognition.

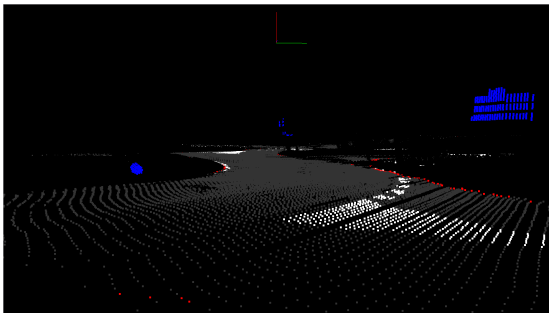

Figure 15: road signs are displayed in blue

4.4 Road markings extraction

With a correctly extracted road and using the reflectivity data, we can also extract road markings trough a simple thresholding. As claimed (Dietmayer et al., 2006), asphalt presents a much lower reflectivity than road markings so that threshold determination is quite easy. Nevertheless, this approach can in some cases be less robust than image processing methods, as it highly depends on marking reflectivity, which is faster deteriorated than white painting.

5 CONCLUSION AND FUTURE WORK

We presented here a new acquisition platform dedicated to road environment reconstruction, surveying and interpretation. Real-

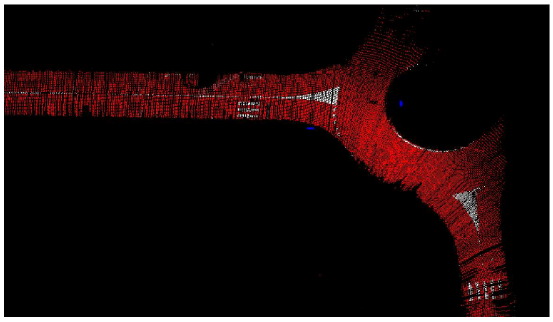

Figure 16: top view of the interpreted 3D environment

istic reconstructions are achieved using multiple 2D lidar sensors and texturized thanks to a lidar / camera cross calibration, when driving at a normal speed.

New algorithm have been developed which can cope with various situations. Road boundaries are detected using a two-step method based on local road shape, which proves to be very precise even on rural roads, where there are no curb. Road sides and main axis are then fitted by arc-length parametrized NURBS, which allow us to compute road width and curvature at the desired resolution. Besides, road markings and traffic signs are extracted using the reflectivity information provided by the lidar sensors ; image processing allow us to interpret these informations. These results are gathered into a geographic information system that can be consulted trough our internal software.

Future works will concern world interpretation, providing information such as road furniture classification, traffic sign aging – using a patented system – or bridge characterization.

REFERENCES

Antone, M. and Friedman, Y., 2007. Fully automated laser range calibration. In: Proceedings of British Machine Vision Conference, Warwick, England, pp. (on CD–ROM).

Aufrere, R., Mertz, C. and Thorpe, C., 2003. Multiple sensor fusion for detecting location of curbs, walls, and barriers. In: Proceedings of the IEEE Intelligent Vehicles Symposium (IV'03), Colombus, OH, USA, pp. (on CD–ROM).

Barber, D., Mills, J. and Smith-Voysey, S., 2008. Geometric validation of a ground-based mobile laser scanning system. ISPRS Journal of Photogrammetry and Remote Sensing 63(1), pp. 128–141.

Boström, G., Fiocco, M., Goncalves, J. and Sequeira, V., 2006. Urban 3d modelling using terrestrial laserscanners. International Archives of Photogrammetry, Remote Sensing and Spatial Information Sciences 36 (Part 5), pp. (on CD–ROM).

Deng, F., Zhang, Z. and Zhang, J., 2004. Construction 3d urban model from lidar and image sequence. ISPRS International Archives of the Photogrammetry, Remote Sensing and Spatial Information Sciences 35 (Part B3), pp. 580–584.

Dietmayer, K., Kämpchen, N., Fürstenberg, K. and Kibbel, J., 2006. Roadway detection and lane detection using multilayer laserscanner. In: Proceedings of International Conference on Robotics and Automation, Orlando, FL, USA, pp. (on CD–ROM).

Fischler, M. A. and Bolles, R. C., 1981. Random sample consensus: A paradigm for model fitting with applications to image analysis and automated cartography. Communications of the ACM 24(6), pp. 381–395.

Früh, C. and Zakhor, A., 2004. An automated method for large-scale, ground-based city model acquisition. International Journal of Computer Vision 60(1), pp. 5–24.

Goulette, F., Nashashibi, F., Abuhadrous, I., Ammoun, S. and Laurgeau, C., 2006. An integrated on-board laser range sensing system for on-the-way city and road modelling. ISPRS International Archives of the Photogrammetry, Remote Sensing and Spatial Information Sciences 36 (Part 1), pp. 43:1–43–6.

Hatger, C. and Brenner, C., 2003. Extraction of road geometry parameters from laser scanning and existing databases. In International Archives of Photogrammetry, Remote Sensing and Spatial Information Sciences 34 (Part 3), pp. 225–230.

Huang, L. and Barth, M., 2008. A novel laser scanner-computer vision mobile sensing system for automatic navigation. In: Proceedings of International Transport System Conference, Beijing, China, pp. (on CD–ROM).

Ishikawa, K., Amano, Y., Hashizume, T., ichi Takiguchi, J. and Yoneyama, S., 2006. Precise road line localization using single camera and 3d road model. In: 23rd International Symposium on Automation and Robotics in Construction, Tokyo, Japan, pp. (on CD–ROM).

Jaakkola, A., Hyyppä, J., Hyyppä, H. and Kukko, A., 2008. Retrieval algorithms for road surface modelling using laser-based mobile mapping. Sensors 8, pp. 5238–5249.

Kim, S.-H., Roh, C.-W., Kang, S.-C. and Park, M.-Y., 2007. Outdoor navigation of a mobile robot using differential gps and curb detection. In: Proceedings of International Conference on Robotics and Automation, Roma, Italy, pp. (on CD–ROM).

Kirchner, A. and Heinrich, T., 1998. Model based detection of road boundaries with a laser scanner. In: Proceedings of the IEEE Intelligent Vehicles Symposium (IV'98), Stuttgart, Germany, pp. 93–98.

Mählisch, M., Schweiger, R., Ritter, W. and Dietmayer, K., 2006. Sensorfusion using spatio-temporal aligned video and lidar for improved vehicle detection. In: Proceedings of Intelligent Vehicles Symposium (IV'06), Tokyo, Japan, pp. (on CD–ROM).

Peterson, J. W., 1992. Arc length parameterization of spline curves. `http://www.saccade.com/writing/graphics/RE-PARAM.PDF`.

Samadzadegan, F., Bigdeli, B. and Hahn, M., 2009. Automatic road extraction from lidar data based on classifier fusion in urban area. In International Archives of Photogrammetry, Remote Sensing and Spatial Information Sciences 38 (Part 3), pp. 81–87.

Sparbert, J., Dietmayer, K. and Streller, D., 2001. Lane detection and street type classification using laser range images. In: 4TH International IEEE Conference on Intelligent Transportation Systems, Oakland, CA, USA, pp. (on CD–ROM).

Talaya, J., Bosch, E., Alamus, R., Serra, A. and Baron, A., 2004. GEOVAN: The Mobile Mapping System from the ICC. ISPRS Book Series, Vol. 4, CRC Press / Balkema, pp. 19–30.

Wijesoma, W. S., Kodagoda, K. R. S. and Balasuriya, A. P., 2004. Road-boundary detection and tracking using ladar sensing. IEEE Transactions on Robotics and Automation 20(3), pp. 456–464.

Zhang, Q. and Pless, R., 2004. Extrinsic calibration of a camera and laser range finder. In: Proceedings of International Conference on Intelligent Robots and Systems, Edmonton, Canada, pp. 2301–2306.

Zhang, Z., 2000. A flexible new technique for camera calibration. IEEE Transactions on Pattern Analysis and Machine Intelligence 22(11), pp. 1330–1334.

Zhao, H. and Shibasaki, R., 2003. Reconstructing a textured cad model of an urban environment using vehicle-borne laser range scanners and line cameras. Machine Vision and Applications 14(1), pp. 35–41.